Friction Coefficient of Slip Critical Bolted Joints with Inorganic Zinc-rich Paint Focusing on Contact Surface Pressure

Ryo Sakura[1*], Yumena Takagi[2], Gen Hayashi[3], and Takashi Yamaguchi[3]
[1*] Division of Civil Engineering, Hokkaido University, Sapporo, Japan.
Kita 13, Nishi 8,Kita-ku, Sapporo, Hokkaido, 060-8628, Japan
(Corresponding author, Ryo Sakura, saaaku022@gmail.com, ORCID 0000-0002-6145-6429)
[2] IHI Infrastructure Systems Co., Ltd., Osaka, Japan.
3 Ohamanishi-machi, Sakai-ku, Osaka-shi, Osaka, 590-0977, Japan
[3] Department of Civil Engineering, Osaka Metropolitan University, Osaka, Japan.
3-3-138 Sugimoto, Sumiyoshi-ku, Osaka-shi, Osaka, 558-8585, Japan

Abstract
Recently, some researchers have reported that the friction coefficient is influenced by the contact surface pressure, and the Coulomb and Amontons' law of friction undergoes breakdown. To develop and apply the bolt that introduces a higher bolt tension to the slip critical bolted joint with the inorganic zinc-rich paint, it is necessary to appropriately evaluate the dependence of the friction coefficient on the contact pressure. This study conducted the friction test, which has various contact surface pressures and application times of contact force, to explore the relationship between friction coefficient and contact surface pressure. The target of faying surface treatment is the inorganic zinc-rich paint coating and blast-cleaned surface, used in slip critical bolted joints of bridges. From obtained results, as the surface pressure increased, the friction coefficient of the inorganic zinc-rich paint case decreased. On the other hand, when the surface pressure varied, the friction coefficient of the blast-cleaned surface case was stable. Considering these slip properties of inorganic zinc-rich paint surfaces, a novel relationship between the friction coefficient and contact surface pressure was proposed. In addition, the theoretical slip strength of bolted joints was calculated using the friction coefficient formulas and the actual contact pressure distribution of the joints. In comparison with the theoretical and experimental slip strength, it was found that the theoretical slip strength calculated based on the proposed friction coefficient formulas depending on contact pressure was closer to the experimental value than that based on the constant friction coefficient and could estimate the tendency of the experimental results.
Keywords: Slip critical bolted joint, Friction coefficient, Slip factor, Inorganic zinc-rich paint

1. Introduction

According to the general design codes, the slip resistance of slip critical joint is determined by bolt tension, slip factor of faying surface, the number of slip planes and bolts. The slip resistance is calculated by Eq. (1).

$$F_s = \mu mnN \tag{1}$$

where μ is the slip factor of faying surface, m is the number of slip planes, n is the number of bolts, and N is the bolt tension. The design slip factor of the slip critical bolted joint is determined by the faying surface condition, not the bolt grade and magnitude of bolt tension. Considering its corrosion resistance and stability performance, the faying surface condition in Japan is selected as the inorganic zinc-rich paint with the shot-blasted cleaned surface. Its slip factor is 0.45 in Japanese Specifications for Highway Bridges (2017).

From an engineering perspective, friction behavior is discussed on the Coulomb and Amontons' law of friction: the friction force is proportional to the loading force and does not depend on the apparent contact area between two solid objects (Coulomb, 1821; Heymanm, 1997). The ratio of the maximum static friction force to the loading force is called the static friction coefficient. Some of the dependencies studied by Coulomb have also been studied in detail in subsequent years, particularly the dependence of the friction coefficient on the contact pressure (Popova et al., 2015; Bijelić et al., 2017). Otsuki et al. reported that the static friction coefficient decreases as a power function of loading force with the power -1/3 of contact force (Otsuki et al., 2013). In addition, it was reported that the friction coefficient and the slip factor of the slip critical joints with aluminum-sprayed plates decreased as the contact pressure increased (Azuma et al., 2016).

In Japan, for the slip critical bolted joint of the steel structure, F10T-M22 friction-type high strength bolts (JIS B 1186, 2018), which is equivalent to ASTM A490 or Grade 10.9(ASTM, 2014; ISO, 2022) and introduce 205 kN is usually used. The design slip factor was determined by the lower bound of the several hundred slip test results using the slip critical bolted joint with F10T bolts. Recently, developing the yield and tensile strength of high strength steel material, the super-high strength bolt which introduces more a higher bolt tension has been developed. For example, 14T super-high strength bolts (hereafter called 14T bolts): the tensile strength is 1,400 ~ 1,600 MPa (Uno et al., 2007) and 1700 MPa-class ultra-high strength bolts (hereafter called 17T bolts) have been developed (Kimura et al., 2007). The design bolt tension of 14T bolts (in M22) is 299kN. However, Mori et al. (2019) reported the slip factor of slip critical bolted joints with 14T bolts and inorganic zinc-rich paint coating was less than the design slip factor because the contact pressure of the faying surface increased due to increasing bolt tension.

If the design slip factor is selected as the current design value (0.45), the design slip resistance of the slip-critical bolted joint using the developed super/ultra-high-strength bolt (14T bolts and 17T bolts) may overestimate the actual slip strength. As the slip critical bolted joint does not allow slippage, it is necessary to quantitatively evaluate the decrease in the slip factor due to the increase in the bolt tension. Although the slip strength of the bolted joint is the summation of the friction force/coefficient on the contact surface, the slip behavior of the slip critical bolted joint is complex due to the uneven contact pressure distribution, as illustrated in Fig. 1. Therefore, the fundamental friction property of the inorganic zinc-rich paint surface is essential. The present study conducted a friction test to evaluate the influence and dependence of the friction coefficient on contact pressure.

In addition, as illustrated in Fig. 2, the inorganic zinc-rich paint has many voids because it is painted by spraying zinc powder and a blinder. It was reported that the thickness of the inorganic zinc-rich paint layer is influenced by the application time and the magnitude of bolt tension (Sakura et al., 2023). Here, the application times of bolt tension mean the time elapsing from bolt tightening to the test start. The friction coefficient and behavior of inorganic zinc-rich paint coating surfaces are expected to be influenced by the application time and magnitude of bolt tension.

In this study, the friction test, which has various contact surface pressures and contact force application times T, was conducted to explore the relationship between friction coefficient and contact surface pressure. Here, the contact force application times mean the time elapsing from applying the horizontal force P_H (see Fig.3) to the test start. The target of faying surface treatment is the inorganic zinc-rich paint coating and blast-cleaned surface used in slip critical bolted joints. Moreover, the theoretical slip strength, calculated based on the uneven distribution of contact surface pressure from FE analysis and developed friction coefficient formulas from the friction test, was compared with the previous test results.

2. Friction tests

2.1. Test program

Friction tests was conducted by the test machine shown in Fig. 3. This test consists of two steps. In the first step, prescribed contact pressure on the contact surfaces of the specimen was introduced by horizontal jack and anchors. In the second step, vertical load was applied until a slip occurred by the testing machine. The prescribed horizontal pressure is retained during the vertical loading. The loading speed is 1kN / sec. The vertical and horizontal loads were measured by 10Hz.
Two types of test specimens were prepared depending on the contact pressure, as shown in Fig. 4. Two specimens with different yield strengths were prepared for the inorganic zinc-rich paint specimen. The material property of Specimen A is SM490Y (Yield strength is 355MPa, and Tensile strength is 490MPa). Specimen B was made by SM570 (Yield strength is 450MPa, and tension strength is 570MPa) so that yielding due to contact pressure would not occur. Here, Wang et al. (2020) reported that the strength grades of steel have presented few influences on the slip behavior of the inorganic zinc-rich paint coating surface. The blast-cleaned specimen was made by SM490Y in the present.
As shown in Table 1, the considered parameters are the type of faying surface treatment and the magnitude of design contact pressure σ_d. As treatments, blast-cleaned surface and inorganic zinc-rich paint coating were prepared. The surface condition of inorganic zinc-rich paint with blast-cleaned surface and blast-cleaned surface is shown in Fig. 5. The surfaces of steel plates are all cleaned to remove rust after the shot blasted by ISO-Sa2 1/2. The design thickness of the inorganic zinc-rich paint is 75 μm. The design contact pressure is between 15 and 450 MPa. There are three or more specimens per case. For the inorganic zinc-rich paint specimen, the contact force application times T are selected as 0, 1, and 3 days, and one month, as shown in Table 2. For the test varying the application time, the contact pressure σ_{slip}, considering the maximum contact pressure of the joints using M22-F10T bolts, was selected as 180 MPa.

2.2. Calculation of contact pressure and friction coefficient

Design contact pressure σ_d is calculated as Eq. (2). In the evaluation of the test results, the measured contact area was used (Eq. (4)).

$$\sigma_d = \frac{P_H}{A_d} \tag{2}$$

Where P_H is the design horizontal load, A_d is the design contact area.
Frictiol coefficient μ_{slip} and contact pressure at slippage σ_{slip} are calculated as Eq. (3) and (4).

$$\mu_{slip} = \frac{P_{V-slip}}{2 \times P_{H-slip}} \tag{3}$$

$$\sigma_{slip} = \frac{P_{H-slip}}{A} \tag{4}$$

Where $P_{V\text{-}slip}$ is vertical load at the slippage, $P_{H\text{-}slip}$ is horizontal load at slippage, A is measured contact area. The actual contact area is measured by the pressure/surface pressure measurement film (Product name is "Prescale" of FUJIFILM). As this friction test evaluates the general friction properties of the interface between two solid bodies, the slip load is defined as the maximum load by the slippage according to ASTM standard G 115(ASTM, 2010), as shown in Fig. 6.

3. Test results

3.1. Influence of contact pressure

Fig. 7 shows the relationship between contact pressure σ_{slip} and friction coefficient μ_{slip}. In addition, the test results of the same test program published by Moriyama et al. (2021) also was written together. Fig. 8 shows the load-relative displacement relationship of one specimen in each case.
As the surface pressure increased, the friction coefficient of the inorganic zinc-rich paint specimen case decreased, as shown in Fig. 7. And the variation of μ_{slip} at $\sigma_{slip} < 45$ and $\sigma_{slip} > 417$ was slight. This is because the increase in multiaxial stress in a layer of inorganic zinc-rich paint has a significant effect. On the other hand, with the variation in contact pressure, the friction coefficient of the blast-cleaned surface case was stable. The difference between this test result and Moriyama et al.'s test results was observed in the blast-cleaned specimen but not in the inorganic zinc-rich paint specimen. The arithmetic average roughness R_a and maximum peak roughness R_Z of specimens in this test were 7 and 41, respectively, and those in Moriyama's test were 12 and 75. Because Moriyama et al.'s test's surface roughness was more rough than this test's, the friction coefficient of the blast-cleaned surface was larger than that of this test. As known from Fig. 7, the friction property of inorganic zinc-rich paint indicated more dependence than the surface roughness.
Fig. 9 and Fig. 10 show the failure modes of the faying surface after the friction test. The inorganic zinc-rich paint

specimen had two types of failure modes. Although the extent of surface damage and wearing differed in the blast-cleaned specimen, the failure mode did not change due to the change in contact pressure. As illustrated in Fig. 11, the friction force consists of furrow force and adhesion force, which are products of interlock action between furrows of faying surface and adhesion effect between contact area, respectively (Carbone et al., 2018; Wang et al., 2020). However, in the inorganic zinc-rich paint specimen, because the faying surface has the paint layer, the friction behavior was affected by the stress triaxiality of the paint layer. As shown in failure modes, up to σ_{slip} =350MPa, the cohesive fracture of inorganic zinc-rich paint occurred, but after that, the interfacial fracture occurred. Therefore, it is considered that the contact pressure dependence of the friction coefficient after σ_{slip} = 350 MPa became smaller. Because the fracture and slippage between the paint layer and steel surface occurred, not the fracture of inorganic zinc-rich paint, the variation of friction coefficient μ_{slip} at σ_{slip} > 417 was slight. And at the range of the cohesive fracture of inorganic zinc-rich paint, the dependence of the friction coefficient on the contact pressure was observed. Generally, the slip factor of bolted joints varies with the timing of surface treatment. However, the influence of the timing of surface treatment was not observed in this friction test because the failure mode of inorganic zinc-rich paint specimens was mainly the cohesive fracture, as shown in Fig. 9.

The relationship between the contact pressure σ and friction coefficient μ_{slip} of the inorganic zinc-rich paint with blast-cleaned surface is proposed as Eq. (5) based on the least squares method. At $\sigma \leq 45$, because the increases of friction coefficient μ_{slip} was not observed, the proposed σ - μ_{slip} relationship is selected as the mean value of the data. At $\sigma \geq 417$, because there is no data and the variation of friction coefficient μ_{slip} is slight, the selected constant value is calculated by Eq. (5).

$$\begin{aligned} \mu_{slip} &= 0.912 && \sigma \leq 45 \\ \mu_{slip} &= 5.604 \times \sigma_d^{-0.477} && 45 < \sigma < 417 \\ \mu_{slip} &= 0.315 && 417 \leq \sigma \end{aligned} \tag{5}$$

Fig. 12 also shows the σ - μ_{slip} relationship of the inorganic zinc-rich paint from Eq. (5) and that of aluminum-sprayed plates Eq. (6) proposed by Azuma et al. (2021). The σ - μ_{slip} relationship of inorganic zinc-rich paint is less than that of aluminum-sprayed. And the slope trend of these curves almost coincides.

$$\begin{aligned} \mu_{slip} &= 4.54 \times 10^{-6}\sigma^2 - 3.38 \times 10^{-3}\sigma + 1.16 && \sigma < 372 \\ \mu_{slip} &= 0.53 && \sigma \geq 372 \end{aligned} \tag{6}$$

3.2. Influence of the contact pressure application time

Fig. 13 shows the friction coefficient μ_{slip}, varying the contact pressure application time T (The contact pressure application time means the time elapsing from applying the horizontal force P_H to the test start.). Fig. 14 shows the load-relative displacement relationship of one specimen in each case.

The lower bound of the friction coefficient μ_{slip} tended to increase with the contact force application time. In addition, the average μ_{slip} did not change until five days but increased by 3% after one month. As shown in Fig. 15, the contact force application time affected the fracture extent of the inorganic zinc-rich paint. As the contact pressure application time increases, the failure and wear of the inorganic zinc-rich paint layer on the contact surface become uniform. The inorganic zinc-rich paint consists of the zinc, the blinder, and the air-fill voids, as illustrated in Fig. 2. It seems that the long-term contact pressure leads to the creep of the blinder, changing the structure of the inorganic zinc-rich paint layer, decreasing the voids, and increasing the density of the paint layer. Thus, the friction coefficient increased slightly when the contact force was continuously applied for one month.

From the above, it seems that the variety of the bolt tension before the slip test and the time from bolt tightening to the slip test influence the slip resistance and coefficient of the bolted joint.

4. Theoretical evaluation for slip strength

The distribution of contact pressure in bolted joints was obtained from FEA, as shown in Fig. 16. The theoretical slip strength was calculated using the friction coefficient from the friction test and the contact pressure distribution of the bolted joints from FEA. In this study, FEA analysis was used only to obtain the contact pressure distribution on the contact surface. The target bolted joints were the two slip test specimens conducted by Mori et al. (2019).

Mori conducted the slip test of the slip critical bolted joints having various bolt tensions (122.7, 169.7, 206.0, 339.7 kN) for the same bolt diameter (M22= 22mm). The surface condition of the specimens was shot blasted by ISO-Sa2 1/2 to remove rust, and the inorganic zinc-rich paint was sprayed with a design thickness of 75 μm. The geometrical configurations of the slip test specimens, which are the edge distance, bolt pitch, width of the plate, thickness of the main plate, thickness of the splice plate, and bolt hole diameter, are 55mm, 80mm, 100mm, 19mm, 12mm, and 24.5mm, respectively. The slip-critical bolted joint consisted of 2 bolts, as shown in Fig. 17. The two strain gauges were attached to the bolt shank on two notched sides to control the magnitude of bolt tension.

In Japan, the slip of the bolted joints is defined by the maximum load or relative displacement (Architectural Institute of Japan, 2021). The former is the maximum load, provided this maximum occurs before a slip displacement of 0.2mm is recorded. The latter is the load corresponding to a relative displacement of 0.2mm. In the slip test of the bolted joints conducted by Mori (2019), the slip load was defined as the maximum load as the slip displacement at the maximum load was smaller than 0.2mm.

For the modeling, a general-purpose structural analysis software, Abaqus/Standard 2020, was utilized to perform three-dimensional elastoplastic finite displacement analysis (Smith, 2020). All the material properties were used in the elastic model. Young's modulus and Poisson's ratio are 200,000 MPa and 0.3, respectively. The mesh size of the main plate and splice plate was set to 1 mm, and that of the High-strength bolt, washer, and nut to 2 mm. The elements applied in the model were three-dimensional-eight-node solid elements with a reduced integration (C3D8R).

In the present study, the selected bolt tension is 206.0 and 340 kN (M22-10T and M22-14T (JIS B 1186, 2018)), which is the magnitude of bolt tension before the test conducted by Mori (2019). Fig. 16 shows the contact pressure distribution between the main and splice plates. The experimental slip strength of these specimens $P_{slip\text{-Exp.}}$ is 450 and 574 kN, as listed in Table 3. The theoretical slip strength was calculated by the piecewise quadrature using the relationship between the friction coefficient - contact surface pressure formula (Eq. (5)) and the contact pressure distribution of the bolted joints (Fig. 16). The coulomb friction coefficient (constant friction coefficient) was selected at 0.55, referring to the experimental results calculated by the slip strength and the magnitude of bolt tension before the test.

Table 3 and Fig. 18 compare with the theoretical and experimental slip strength. The theoretical strength based on the Coulomb friction (constant friction coefficient) coincides with the 10T bolt case test result and overestimates about 20% that of the 14T bolt case. On the other hand, the theoretical strengths based on Eq. (5) are on the safe side of the test results for both 10T and 14T bolt cases. It was found that Eq (5) can evaluate the same tendency of the test results, which decreases the slip factor due to the increase of the bolt tension. This is because the proportion of high contact pressure in the 14T bolt case was more extensive, and the friction coefficient around the bolt hole was lower than in the 10T bolt case (see Fig. 16). In this study, the theoretical value calculated by Eq. (5) could estimate the tendency of the experimental results but not match the absolute value. This is because it seems that Eq. (5) was based on only the least squares method. In future work, it is necessary to develop the calibration method of the friction coefficient function to estimate the experimental value by considering the variation of the friction coefficient.

From the above, it was found that the friction property of the inorganic zinc-rich paint surface had a negative correlation at the area of high contact pressure, and the possibility that decreasing the slip factor for the slip-critical bolted joint with the ultra/super-high-strength bolt is necessary.

5. Conclusions

This study aimed to clarify the relationship between friction coefficient μ_{slip} and contact surface pressure σ_{slip} at the contact surface of slip critical bolted joints. For this purpose, a friction test was conducted. The obtained concluding remarks are as follows.

(1) As the surface pressure increased, the friction coefficient μ_{slip} of the inorganic zinc-rich paint case decreased. When the fracture of inorganic zinc-rich paint (cohesive fracture) caused the slippage, the relationship between contact pressure σ_{slip} and friction coefficient μ_{slip} had a negative correlation. On the other hand, when the slippage between the paint layer and the steel surface (interfacial fracture) caused the slippage, the variation of friction coefficient μ_{slip} was slight. Considering these slip properties of inorganic zinc-rich paint, a novel relationship between friction coefficient and contact surface pressure of the inorganic zinc-rich paint surface was proposed (Eq. (5)).

(2) The friction coefficient μ_{slip} of the blast-cleaned surface case was stable. On the other hand, μ_{slip} of the blast-cleaned surface was affected by the surface roughness. Therefore, the slip property of inorganic zinc-rich paint has more dependence than the surface roughness.

(3) Using the friction coefficient formulas (Eq. (5) and coulomb friction) and the actual contact pressure distribution of the bolted joints from FE analysis, the theoretical slip strength of bolted joints was calculated. The theoretical strengths based on Eq. (5) were on the safe side of the test results for both 10T and 14T bolt cases. It was found that Eq. (5) can evaluate the same tendency of the test results, which decreases the slip factor due to the increase of the bolt tension. However, the theoretical strength based on the Coulomb friction (constant friction coefficient) was overestimated by about 20% in the 14T bolt case.

(4) The average of friction coefficient μ_{slip}, varying the application time of contact pressure, did not change until 5 days but increased slightly when the contact force was continuously applied for one month.

This study found that decreasing the slip factor for the slip-critical bolted joint with the ultra/super-high-strength bolt that occurs high contact pressure may be necessary. In addition, the variation in slip factor is significant due to the variation of the bolt tension, the anchor pattern of the steel plate, and the thickness of the paint. Therefore, to define the design slip factor of the slip-critical bolted joint of super/ultra-high-strength bolts, further data accumulation of the test results of bolted joints and statistical evaluation of the slip factor and the friction coefficient are needed in future works.

Acknowledgements
This work was supported by the Maeda Engineering Foundation and the SPRING program of the Japan Science and Technology Agency (JST SPRING, Grant Number JPMJSP2139).

References

JRA (Japan Road Association), Specifications for Highway Bridges Part II Steel Bridges, 2017.

Coulomb C A. “Theorie des machines simple (Theory of simple machines).” Bachelier, Paris, 1821.

Heyman J. “In Coulomb’s Memoir on Statics. An Essay in the History of Civil Engineering.” London: Imperial College Press, 1997: 212.

Popova, E. and Popov, V. L. “The research works of Coulomb and Amontons and generalized laws of friction.” Friction 3, 183–190, 2015.

Bijelić, I., Mor, N., Živković, M., Tubin, V., Stožinić, T. “The Influence of the Contact Pressure on the Value of the Coefficient of Friction”, Tribology in Industry, Volume 39, No 2, pp. 255-259, 2017. https://doi.org/10.24874/ti.2017.39.02.13

Otsuki, M. and Matsukawa, H. “Systematic breakdown of Amonton’s law of friction for a elastic object locally obeying to Amonton’s law.” Sci. Rep. 3, 1586, 2013.

Azuma, K. and Kumai, T. “A study on the averaged values of contact pressure and friction coefficient of bolted friction joints with aluminum-sprayed steel splice plates.” Journal of steel construction engineering, Vol. 23, No. 90, pp. 117-131, 2016. (**in Japanese**)

ASTM, Standard Specification for Structural Bolts, Alloy Steel, Heat Treated, 150 Ksi Minimum Tensile Strength, American Society for Testing and Materials International, 2014.

ISO, ISO 4014: Fasteners - Hexagon Head Bolts - Product Grades a and B, International Organization for Standardization, Switzerland, 2022.

UNO, N., KUBOTA, M., NAGATA, M., TARUI, T., KANISAWA, H., YAMASAKI, S., AZUMA, K., MIYAGAWA, T., “Super High Strength Bolt “SHTB®””, Nippon Steel Technical Report , No.387,pp.85-93, 2007. (**in Japanese**)

Kimura, Y., Masuda, H., Yamaguchi, T., Nagasaki, E., Moriyama, H., Tsuzaki, K.: Influence of Bolt Shape and Dimensions on Mechanical Property of 1700 Mpa-Class Ultra-High Strength Bolt, Steel Construction Engineering, Vol.27 No.107, 2020, https://doi.org/10.11273/jssc.27.107_41 (**in Japanese**)

Mori, T., Amitani, T., Uchida, D. “Influence of Bolt Tightening Force on Slip Coefficient of High-Strength Bolted Friction Type Joints”, Journal of Japan Society of Civil Engineers, Ser. A1 (Structural Engineering & Earthquake Engineering (SE/EE)), Volume 75, Issue 1, pp. 58-66, 2019, https://doi.org/10.2208/jscejseee.75.58 (**in Japanese**)

Sakura, R., Sugimoto, Y., Sakai, T., Yamaguchi, T., Kitane, Y., Mitsugi, Y. “Influence of tightening bolt load and bolt load before test on slip resistance properties of inorganic zinc rich paint of friction type bolted joint”, Journal of Structural Engineering, A, Volume 69A, pp. 442-450, 2023.https://doi.org/10.11532/structcivil.69A.442 (**in Japanese**)

Wang, Y., Wang, Y., Chen, K., Jin, H., “Slip factor of high strength steel with inorganic zinc-rich coating”, Thin-Walled Structures, Volume 148, 106595, 2020, https://doi.org/10.1016/j.tws.2019.106595.

Standard Guide for Measuring and Reporting Friction Coefficients, ASTM Standard G 115, 2010.

Moriyama, H., Sakura, R., Yamaguchi, T. Takai, T. and Yamamoto, Y. “Exploration of Novel Faying Surface Treatment for High-Strength Frictional Bolted Joints to Enhance its After-Slip Performance.” IABSE Congress Ghent, pp. 1684-1691, 2021. https://doi.org/10.2749/ghent.2021.1684

A.I. Vakis, V.A. Yastrebov, J. Scheibert, L. Nicola, D. Dini, C. Minfray, A. Almqvist, M. Paggi, S. Lee, G. Limbert, J.F. Molinari, G. Anciaux, R. Aghababaei, S. Echeverri Restrepo, A. Papangelo, A. Cammarata, P. Nicolini, C. Putignano, G. Carbone, S. Stupkiewicz, J. Lengiewicz, G. Costagliola, F. Bosia, R. Guarino, N.M. Pugno, M.H. Müser, M. Ciavarella, “Modeling and simulation in tribology across scales: An overview”, Tribology International, Volume 125, pp. 169-199, 2018, https://doi.org/10.1016/j.triboint.2018.02.005.

M. Smith, ABAQUS/Standard User’s Manual, Version 2020, Dassault Systèmes Simulia Corp, Providence, RI, 2020.

JIS B 1186: Sets of high strength hexagon bolt, hexagon nut and plain washers for friction grip joints, 13th Edition, Japan Industrial Standards committee, 2018.

Architectural Institute of Japan, “Recommendation for Design of Connections in Steel Structures”, 2021

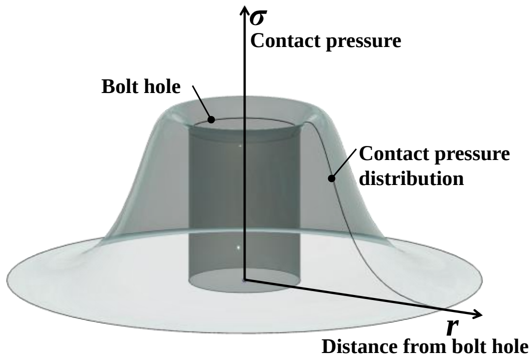

Fig. 1 Contact pressure distribution of the bolted joint

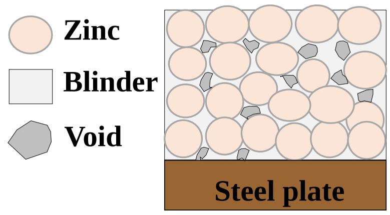

Fig. 2 Conformation of inorganic zinc-rich paint

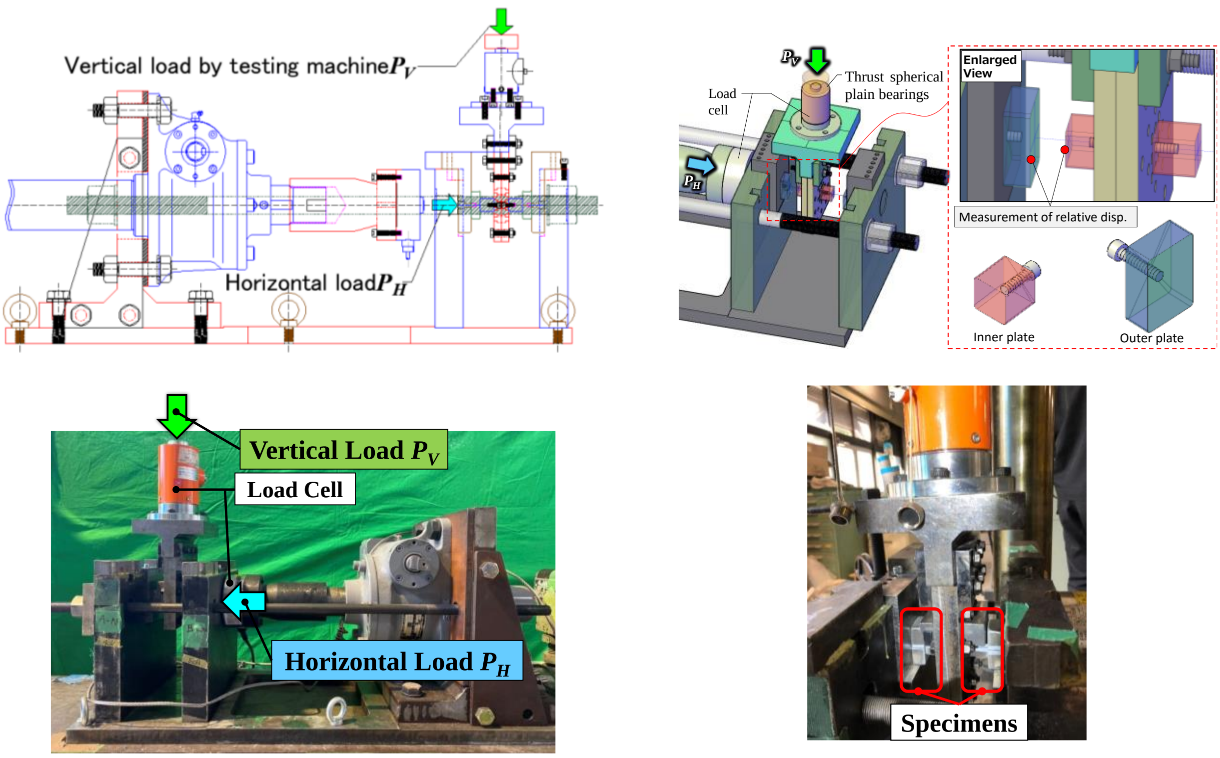

(a) Plane view (b) Test set-up

Fig. 3 Schematic illustration and picture of testing machine and test set-up

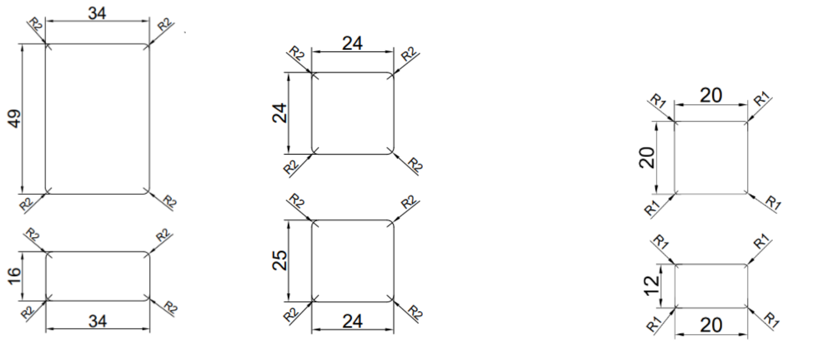

Inner plate　　Outer plate　　Inner and outer plate

Specimen A　　Specimen B

Fig. 4 Dimensions of specimens (unit: mm)

Inorganic zinc-rich paint coating surface　　Blast-cleaned surface

Fig. 5 Faying surface condition of the specimen

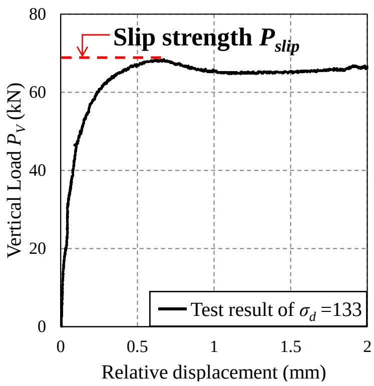

Fig. 6 Definition of slip strength

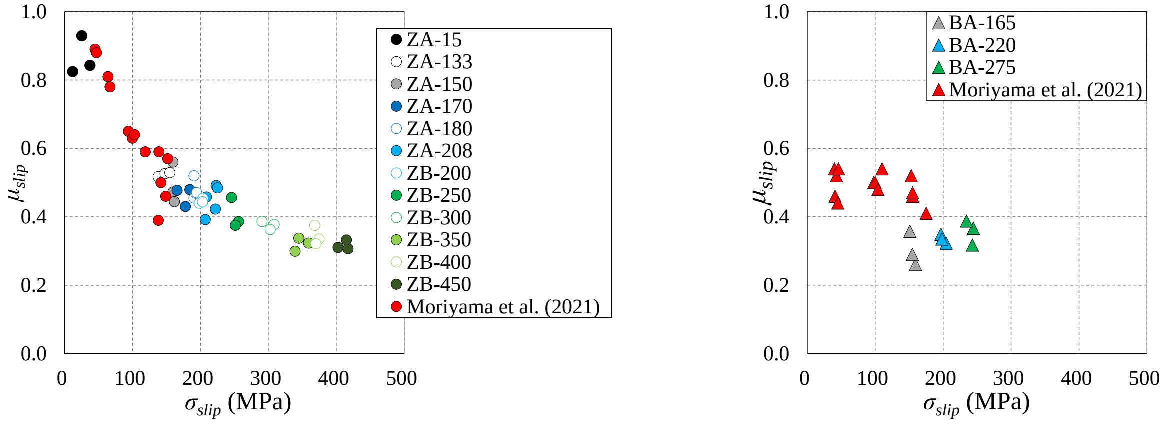

Inorganic zinc-rich paint coating surface

Blast-cleaned surface

Fig. 7 Relationship between friction coefficient μ_{slip} and contact pressure σ_{slip}

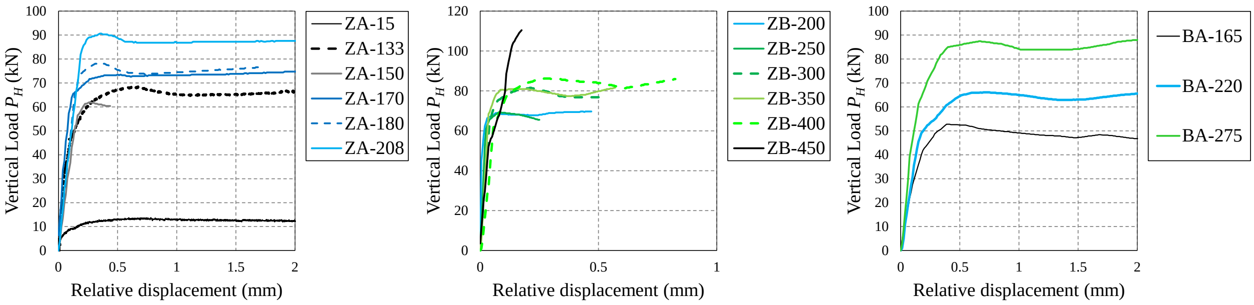

Fig. 8 Relationship between load vs. displacement

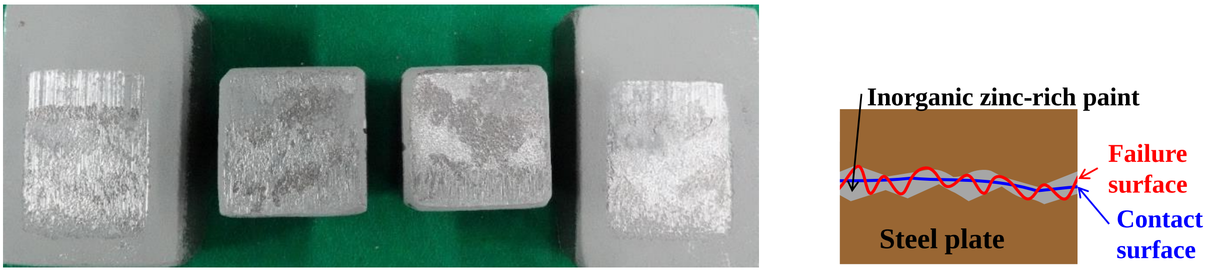

(a) Cohesive fracture at σ_{slip} = 200 MPa

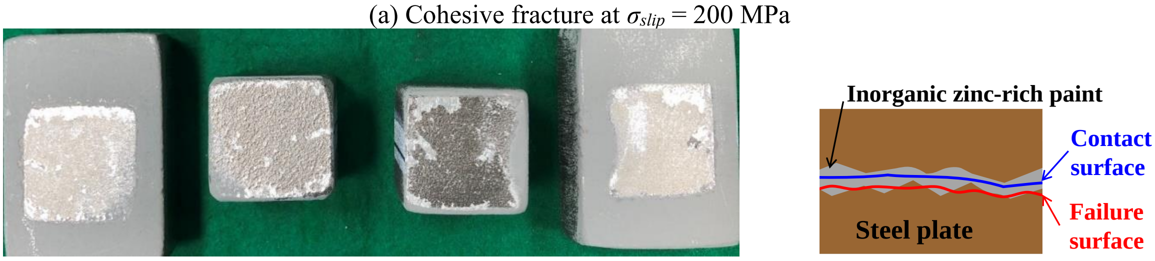

(b) Interfacial fracture at σ_{slip} = 350 MPa

Fig. 9 Failure modes of inorganic zinc-rich paint

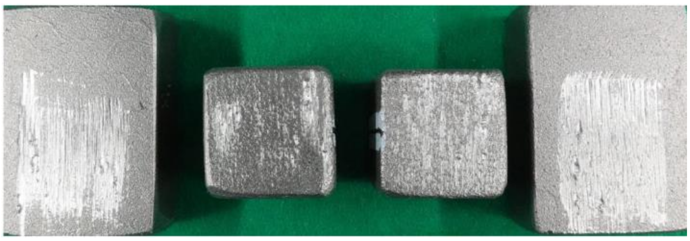

(a) At σ_{slip} = 155 MPa

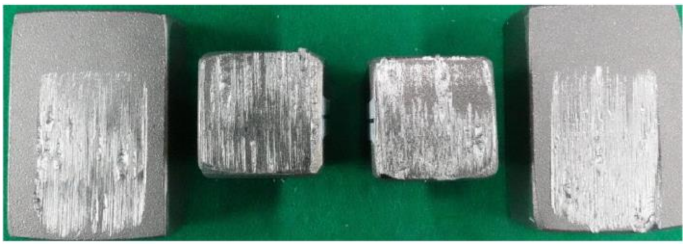

(b) At σ_{slip} = 250 MPa

Fig. 10 Failure modes of Blast-cleaned surface

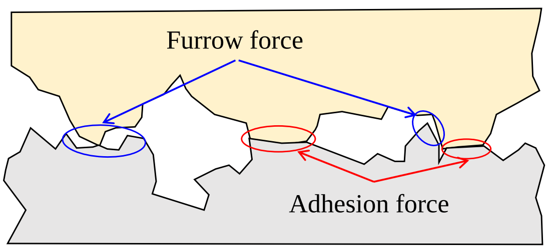

Friction force =Furrow force + Adhesion force

Fig. 11 Friction model between two slid bodies

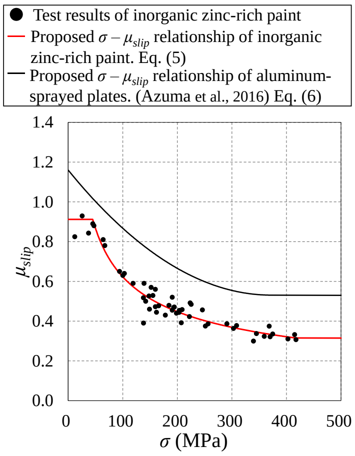

Fig. 12 Proposed $\sigma - \mu_{slip}$ relationship

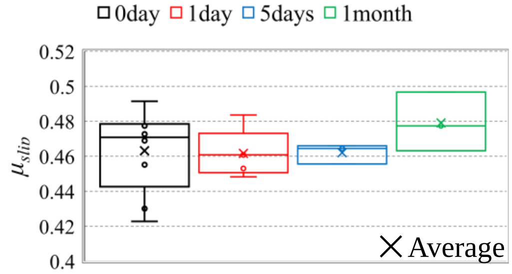

Fig. 13 Influence of the contact pressure applying time

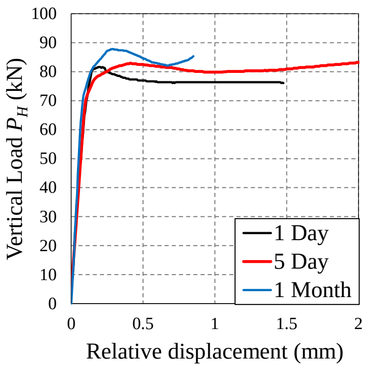

Fig. 14 Relationship between load vs. displacement

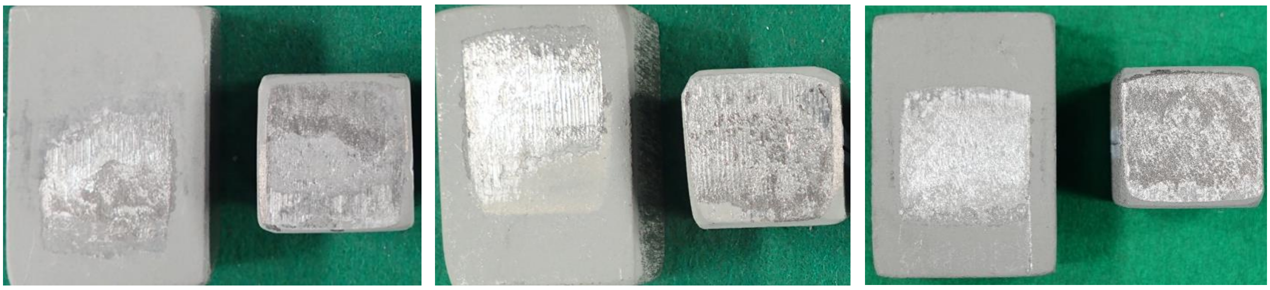

(a) 1 Day (b) 5 Day (c) 1 Month

Fig. 15 Influence of the contact pressure applying time for the failure mode

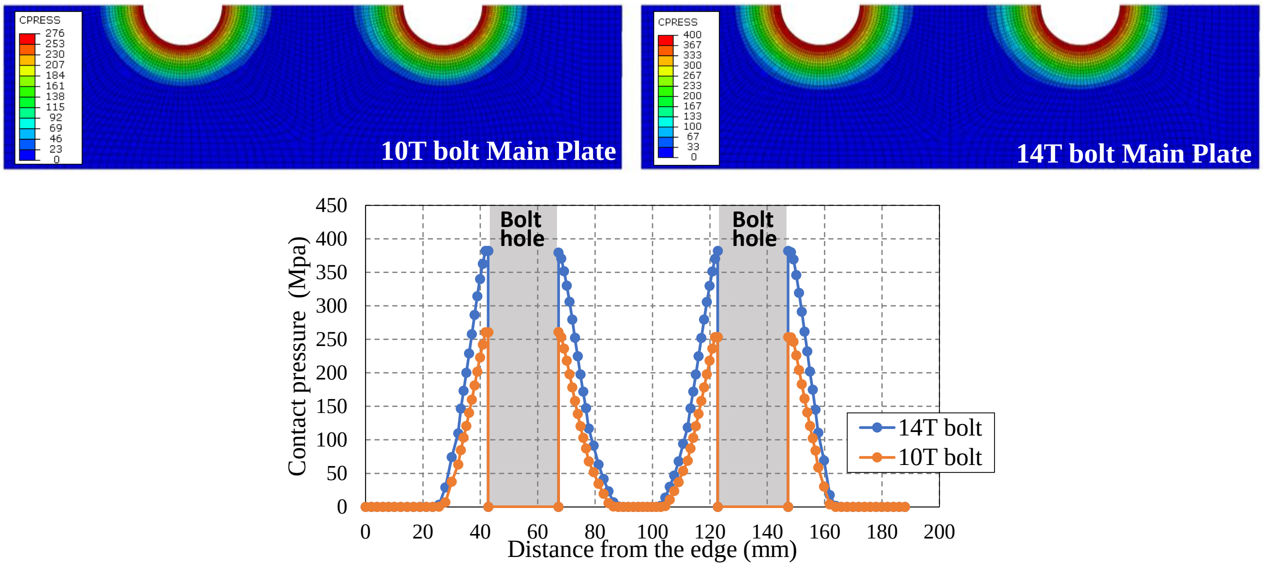

Fig. 16Contact pressure distribution between the main and splice plate

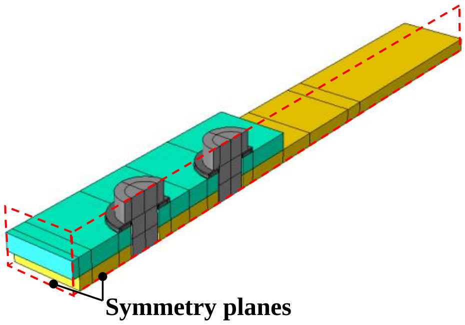

Fig. 17 Overall view of FE model

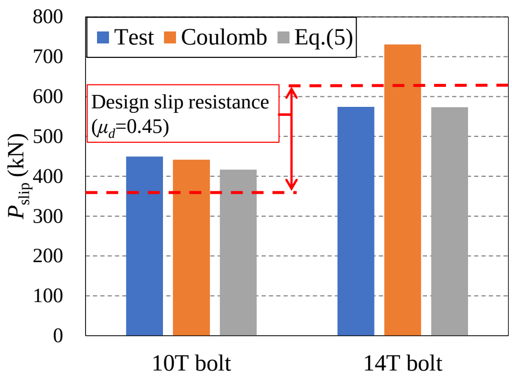

Fig. 18 Comparison with theoretical and test slip strength

Table 1 Summary of friction test specimens

Specimen name	Faying Surface treatment	Specimen shape type (Fig. 4)	Design Contact Area A_d (mm^2)	Design Contact Pressure σ_d (MPa)	Design Horizontal Load P_H (kN)
ZA-15	Inorganic zinc-rich paint with blast-cleaned surface	A	480	15	8
ZA-133				133	70
ZA-150				150	79
ZA-170				170	90
ZA-180				180	95
ZA-208				208	110
ZB-200		B	400	200	83
ZB-250				250	104
ZB-300				300	123
ZB-350				350	144
ZB-400				400	163
ZB-450				450	183
BA-165	Blast-cleaned	A	480	165	79
BA-220				220	106
BA-275				275	132

Table 2 Application time of horizontal load

Application Time	n	σ_d (MPa)	P_H (kN)
0 Day	7	180	95
1 Day	5		
5 Days	3		
1 Month	3		

Table 3. Estimation of the slip strength

Specimen name	Test results (Mori et al.) (Average of 3 specimens)			Design resistance	Theoriotical evaluation results					
					Coulomb friction μ=0.55			Eq. (5)		
Bolt grade	Bolt tension before test $N_{0\text{-Exp.}}$ (kN)	Slip strength $P_{\text{slip-Exp.}}$ (kN)	Slip factor $\mu_{\text{slip-Exp.}}$	Slip resistance from Eq.(1) (μ_d=0.45)	Slip strength $P_{\text{slip-FE1}}$ (kN)	$P_{\text{slip-Exp.}}$ / $P_{\text{slip-FE1}}$	Slip factor $\mu_{\text{slip-FE1}}$	Slip strength $P_{\text{slip-FE2}}$ (kN)	$P_{\text{slip-Exp.}}$ / $P_{\text{slip-FE2}}$	Slip factor $\mu_{\text{slip-FE2}}$
10T bolt	412	449.7	0.55	370.8	441.5	1.02	0.54	416.6	1.08	0.51
14T bolt	680	574.3	0.42	612.0	730.7	0.79	0.54	573.5	1.00	0.42
14T / 10T	-	1.28	0.77	1.65	1.65	-	1.00	1.38	-	0.83